Sr ion distribution and local structure in $La_{1-x}Sr_xMnO_3$

2006 J. Phys.: Condens. Matter 18 5579

(http://iopscience.iop.org/0953-8984/18/23/026)

INSTITUTE OF PHYSICS PUBLISHING JOURNAL OF PHYSICS: CONDENSED MATTER

J. Phys.: Condens. Matter **18** (2006) 5579–5586 doi:10.1088/0953-8984/18/23/026

Sr ion distribution and local structure in $La_{1-x}Sr_xMnO_3$

F L Tang, X Zhang[1] and Y Shao

Laboratory of Advanced Materials, Department of Materials Science and Engineering, Tsinghua University, Beijing 100084, People's Republic of China

E-mail: xzzhang@tsinghua.edu.cn

Received 13 February 2006, in final form 21 April 2006
Published 26 May 2006
Online at stacks.iop.org/JPhysCM/18/5579

Abstract

Atomic simulation is performed on $La_{1-x}Sr_xMnO_3$ ($x = 1/18, 1/9, 1/6, 2/9$ and $1/4$) to study the Sr ion distribution and local structure. Our calculation reveals a tendency for Sr clustering rather than a random Sr distribution. It is found that local structures in the vicinity of the La and Sr clusters are different. The existence of local structural difference indicates a nano-scale structural inhomogeneity, which may lead to electronic structure inhomogeneity. We expect that such a cation distribution may be a compositional representation of magnetoelectronic phase separation.

1. Introduction

The manganite-based magnetoresistive oxides such as $La_{1-x}D_xMnO_3$ (where D is a divalent cation such as Ca, Sr or Ba) have been investigated intensively due to their rich display of interesting basic-physics problems and possible applications [1–3]. Some earlier studies indicated that the electronic/magnetic inhomogeneity or phase separation in these compounds may be to atomic distributions and different local structure [1, 4].

In $La_{1-x}Sr_xMnO_3$, Shibata *et al* [5] found structural disorder on the cation sublattice in low-x samples, and indicated a tendency for Sr clustering by fitting their experimental data. Louca and Egami [6] showed a clear departure of the actual local structure from the average crystallographic structure in $La_{1-x}Sr_xMnO_3$ ($0 \leqslant x \leqslant 0.5$). The difference of the MnO_6 octahedron in the charge-rich and charge-poor regions was found to be notable in terms of the local Jahn–Teller (JT) distortion. A coexistence of antiferromagnetism and ferromagnetism was found in (La, Sr)Mn_2O_7 and was attributed to local lattice distortion, suggesting a large local deviation from the average lattice [7]. The phase separation with electron-rich and electron-poor regimes had a lower energy than an antiferromagnetic phase with uniform density [8]. In $La_{1-x}Ca_xMnO_3$ ($x = 0.05, 0.08$), a pattern of hole-rich magnetic clusters with a hole-poor

[1] Author to whom any correspondence should be addressed.

Table 1. Potential parameters for $SrMnO_3$: short-range interaction and shell-model parameters. Potential parameters for Mn^{4+}–O^{2-} and O^{2-}–O^{2-} are the same as that in $CaMnO_3$ [15].

	Short-range interaction		
	A (eV)	ρ (Å)	C (eV Å^6)
Sr^{2+}–$O(1)^{2-}$	22 956.7020	0.2356	0.0
Sr^{2+}–$O(2)^{2-}$	40 452.3757	0.2252	0.0
	Shell-model parameters		
Species	Y (e)	K (eV Å^{-2})	
Sr^{2+}	1.831	21.53	

medium was detected [9]. It was suggested that the phase separation gives rise to small domains of low hole density surrounded by a background of high density. In these domains, Jahn–Teller deformations will be favoured [10].

Although many studies have revealed the possible relation between phase separation, atomic distribution, and different local structure in these materials, the details of how the La-site cations distribute themselves in the local structure are not clear. In this paper, we use an atomistic simulation technique to study the possible Sr cation distribution and local structure in $La_{1-x}Sr_xMnO_3$ ($x = 1/18, 1/9, 1/6, 2/9$ and $1/4$) at 0 K.

2. Computational methods

Our atomistic simulation technique, based on the widely used successful Bohn core–shell model, can predict the crystal structure of a material at a given temperature and pressure by minimizing its free energy. It has been used for simulating many kinds of compounds [11–15]. A brief illustration of this technique can be referred to in [15], and details are available in [12].

It should be stressed that the reliability of our simulation strongly depends on the validity of the potential model used, and the latter is assessed primarily by its ability to reproduce experimental crystal properties. The potential parameters used for $LaMnO_3$ had been fitted, which can reproduce the experimental crystal structure of $LaMnO_3$ well, with the differences in lattice parameters between the calculated and experimental data less than 1% [15]. The newly fitted potential parameters of $SrMnO_3$ are given in table 1. The differences in lattice parameters and bond lengths of $SrMnO_3$ between calculated and experimental data are less than 0.001 Å [16].

We had further examined the validity of our potential model for $LaMnO_3$ by calculating the pressure effect on the lattice parameters of $LaMnO_3$ up to 3.4 GPa. The calculated compressibility is in agreement with the experimental value, indicating that the potentials that we used can represent the crystal structure of $LaMnO_3$ [15].

We had investigated the vibrational contributions of Sr-doped $LaMnO_3$ at low temperatures in order to further check the validity of $SrMnO_3$'s potential parameters. For studying the temperature effect on the lattice parameters and bond lengths, one converged configuration of $La_{5/6}Sr_{1/6}MnO_3$ was heated from 0 to 75 K. It was found that the lattice parameters and Mn–O bond lengths (figure 1) are almost unchanged when the temperature increases, which is consistent with the experimental results [17]. This vibrational check indicates that our $SrMnO_3$ potentials are stable and suitable for the simulation of Sr-doped $LaMnO_3$ at low temperatures less than 75 K. The above lattice, pressure, and temperature effect tests indicate that our potentials can represent the crystal structures of $La(Sr)MnO_3$.

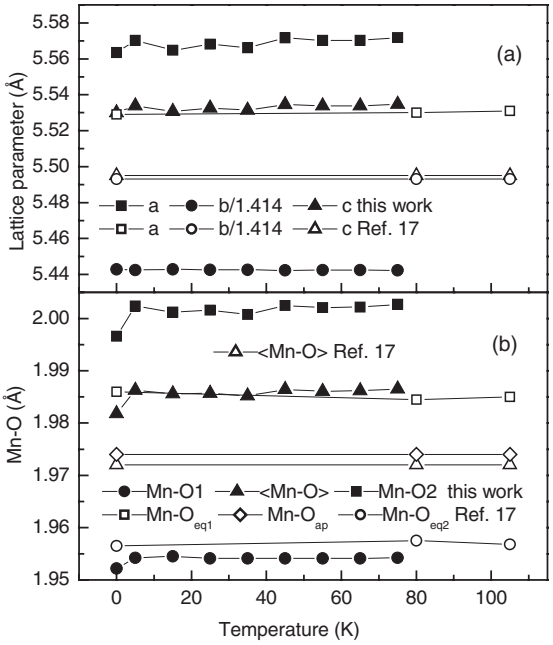

Figure 1. Temperature dependence of lattice parameters (a) and Mn–O bond length (b) in $La_{5/6}Sr_{1/6}MnO_3$. We denote the O^{2-} ions along the *b*-axis as O1, and the O^{2-} ions on the *a*–*c* plane as O2 in an MnO_6 octahedron. Experimental results of [17] are obtained from $La_{0.835}Sr_{0.165}MnO_3$, and there are two nonequivalent oxygen positions, apical (O_{ap}) and equatorial (O_{eq1} and O_{eq2}), which characterize distortion of the MnO_6 octahedron in terms of lengths of the Mn–O bonds. $\langle\,\rangle$ denotes the average value.

In this work, the initial structure for studying doped $LaMnO_3$ is the crystallographic unit cell of $LaMnO_3$, which has four La^{3+} ions, four Mn^{3+} ions, four O1 ions and eight O2 ions. To meet the demand of the Sr-doping ion number proportion and make the calculations most efficient, the unit cell of $LaMnO_3$ is extended three times along both the *a*- and *c*-axis directions. There are 36 La^{3+}, 36 Mn^{3+} and 108 O^{2-} ions in the extended supercell. For simulating the structure of $La_{1-x}Sr_xMnO_3$, $36x$ La^{3+} and $36x$ Mn^{3+} ions are substituted by Sr^{2+} and Mn^{4+} ions, respectively.

The size effect in simulation has also been considered. For different sizes of the supercell of $LaMnO_3$ containing 4, 9, and 16 unit cells, the variation in lattice energy is less than 0.001 eV and the variation in lattice parameters is less than 0.001 Å. At $x = 1/4$, some simulations of Sr-cluster doping are carried out with the above three types of supercell. It is also found that the variation in average lattice energy (<0.01 eV) and the variation in average lattice parameter (<0.002 Å) are also small. Therefore, the supercell size has little effect in our simulation.

3. Results and discussion

3.1. Lattice transition and local structures

Two kinds of calculations were performed at 0 K. One was performed on the configurations with a random distribution of Sr ions, and the other on the configurations with an Sr cluster distribution. At every doping level, about 300–500 random configurations and 16–120 cluster configurations are simulated. For most of the random configurations, their lattice energies

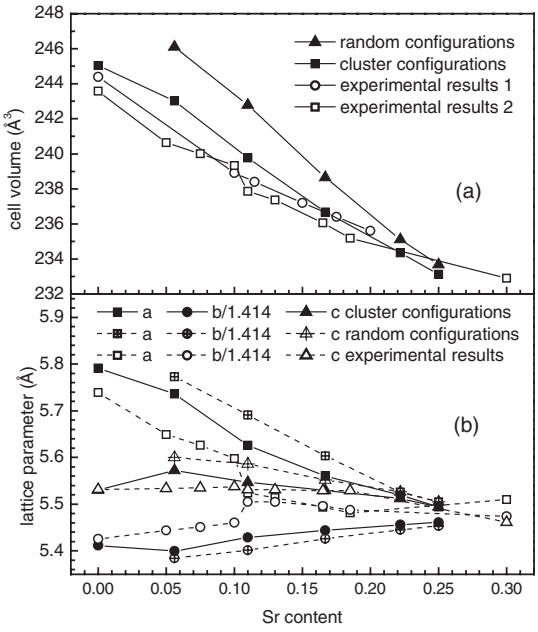

Figure 2. Comparison of calculated and observed cell volume (a), and lattice parameters (b) in $La_{1-x}Sr_xMnO_3$. Experimental volumes of results 1 are abstracted from [18]. Experimental volumes of results 2 and lattice parameters are abstracted from [15] ($x = 0$), [19] ($x = 0.05, 0.075$ and 0.1), [17] ($x = 0.11, 0.13, 0.165$ and 0.185), and [20] ($x = 0.3$). Experimental data were measured at different temperature (>0 K).

cannot converge. Their calculated lattice parameters deviate from experimental values a great deal. But, for almost all the cluster configurations, their lattice energies converge and their calculated lattice parameters deviate from experimental values just a little. At every doping density, 10 random configurations with the least deviation from the experimental results are taken into account for comparison. The comparison between the average results of all the converged cluster configurations, selected random configurations (with the least deviations from experimental results) and some experimental results is shown in figure 2.

From figure 2, one can find that the results of the cluster configuration are closer to the experimental results [17–20] than the results of the random configurations, indicating that the cluster configurations are more structurally reasonable than the random configurations. It is also found that, as the doping density increases, the calculated cell volume decreases, the calculated lattice parameter a decreases significantly, and b increases little, but c remains almost unchanged. At every doping density, the average lattice energy of cluster configurations is slightly lower than that of random configurations by about 0.05–0.1 eV per cell, indicating that the cluster configurations are slightly more energetically favourable than the random configurations.

The local disorders around La/Sr site are found not to be homogeneous. The eight La/Sr–Mn bond lengths at every doping density are shown in figures 3(a) and (b). It is found that the average La–Mn bond length is slightly smaller than the average La–Mn bond length in $LaMnO_3$. But the average Sr–Mn bond length is larger than the Sr–Mn bond length in $SrMnO_3$. The average bond length of La–Mn is always larger than the Sr–Mn bond length at every doping density under study. In addition, the variation between Sr–Mn bond lengths is smaller than

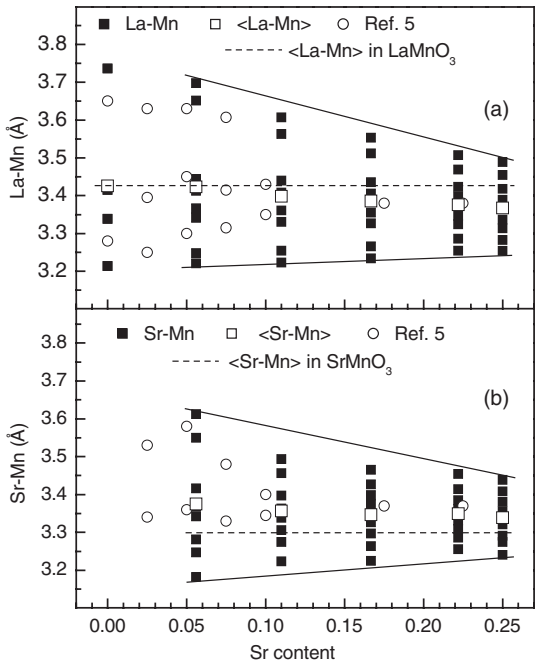

Figure 3. The La–Mn (a) and Sr–Mn (b) distances as a function of doping densities x at 0 K. $\langle\,\rangle$ denotes the average value.

that among La–Mn bond lengths. Hence, in the vicinity of the clustered Sr^{2+} ions, the local structural disorders are significantly smaller than those in the vicinity of La^{3+} ions, and the local structure disorders in the vicinity of the clustered Sr^{2+} and La^{3+} ions are reduced by increasing the doping densities x. This result supports the experimental result of [5], which revealed a consistent deviation from a random Sr distribution at the La/Sr sites for $x \leqslant 0.3$, and the local structure distortions are reduced by increasing x.

The different local structure can also be illustrated using Mn–O bond lengths in Sr-doped $LaMnO_3$. In figure 5(d) (one of the typical Sr-cluster configurations of $La_{5/6}Sr_{1/6}MnO_3$), there are four Mn^{3+} and two Mn^{4+} ions along the arrow line in the Mn–O2 plane. The six Mn–O bond lengths of each Mn ion are shown in figure 4(a). It is found that the average Mn^{3+}–O bond length is larger than the average Mn^{3+}/Mn^{4+}–O bond length and is very close to the average Mn^{3+}–O bond in $LaMnO_3$. But the average Mn^{4+}–O bond length is smaller than the average Mn^{3+}/Mn^{4+}–O bond length and is very close to the Mn^{4+}–O bond in $SrMnO_3$. Figure 4(b) shows the Jahn–Teller distortion (see [21] for the calculation method) of every Mn ion. The Jahn–Teller distortion around Mn^{3+} ions is smaller than that in $LaMnO_3$, whereas the distortion around Mn^{4+} ions is very small but larger than that in $SrMnO_3$. Our calculation confirms that the lattice distortions are concentrated on the Jahn–Teller distorted $Mn^{3+}O_6$ octahedra, and that almost no distortion occurs on the $Mn^{4+}O_6$ octahedra. This result agrees with that in [6, 18] and [19].

The structural transition can affect the electronic/magnetic properties of doped manganites. When Sr ions are doped into manganites, both lattice distortion (figure 2) and MnO_6 octahedral distortion (Jahn–Teller distortion for $Mn^{3+}O_6$, not shown) will reduce when the doping density increases from 0 to 1/4. On the one hand, these structural transitions in Mn–O bond lengths and Mn–O–Mn bond angles can lead to different e_g electron hopping integrals by the mechanism

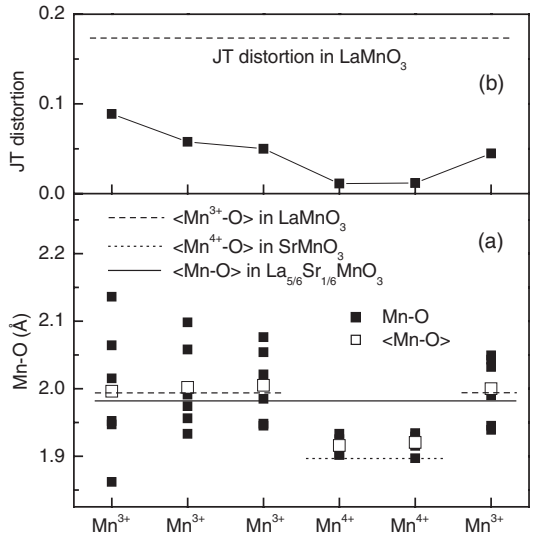

Figure 4. The Mn–O (a) bond lengths and Jahn–Teller distortion (b) of some MnO_6 octahedra in figure 5(d). $\langle\,\rangle$ denotes the average value.

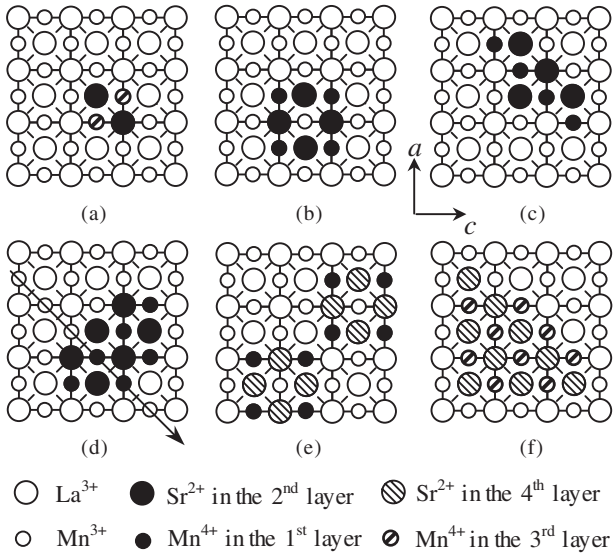

Figure 5. Some typical cluster configurations of $La_{1-x}Sr_xMnO_3$ at $x = 1/18$ (a), $1/9$ ((b), (c)), $1/6$ (d), $2/9$ (e) and $1/4$ (f). The number of the layer denotes the sequential order of the MnO_2 or LaO layer along the b direction. O^{2-} ions are not shown.

of double exchange, i.e. the bandwidth is changed (see [21] for the method for calculating the bandwidth from bond lengths and bond angles). On the other hand, the doping results in local structural transition, for example, JT polaron distortion energy (relating to the strength of electron–phonon coupling) is also changed [21]. Then, magnetic properties, such as T_C, can be changed by the changes in bandwidth and JT energy [22].

3.2. Sr clusters and phase separation

Our simulation indicates that Sr ions have the structural possibility and a small thermodynamic tendency to clustering at low temperatures. Some typical Sr cluster distributions at different doping densities are shown in figure 5. It is found that Sr^{2+} ions form a cluster on the length scale of 5–15 Å: Sr^{2+} ions are always surrounded by Mn^{4+} ions, and Sr^{2+} and Mn^{4+} ions locate in two adjacent layers along the *b*-direction. Our calculation also manifests that the configurations with separated Sr^{2+} and Mn^{4+} ions are always structurally unreasonable. The adjacency of Sr^{2+} and Mn^{4+} ions forms a chemical inhomogeneity, similar to the $SrMnO_3$ structure, surrounded by a background of the $LaMnO_3$ structure. These clusters will introduce a local structure deviation. This chemical inhomogeneity and local structure deviation may lead to electronic structure inhomogeneity, which can affect magnetic and electronic properties of this compound [5].

Our simulated Sr clusters are consistent with some experimental suspicions. A tendency for Sr clustering was observed in lightly doped $La_{1-x}Sr_xMnO_3$ [5]. The local structure disorder in the vicinity of the clustered Sr ions was significantly smaller than that in the vicinity of La ions, presumably attributed to a higher average Mn^{3+} concentration near the La regions. In $La_{0.7}Ca_{0.3}MnO_3$, two spatially separated regions ($\leqslant$30 Å) have been found, and this spatial inhomogenity was suspected to be related to the distribution of La and Ca ions and the corresponding fluctuation in the local lattice distortions [23]. We believe that such chemical inhomogeneity, along with the different local structure, will be crucial to the theoretical study of these compounds, particularly in the context of magnetoelectronic phase separation.

Our simulated Sr clusters have a length scale of 5–15 Å, which is similar to some experimental values of microscopic-sized clusters (or droplets, or domains). Teresa *et al* detected the spontaneous formation of localized $\sim$12 Å magnetic clusters in $(La–Y/Tb)_{2/3}Ca_{1/3}MnO_3$ [24]. Hennion *et al* revealed the isotropic droplets of about 9 Å in electronic phase separation [9]. Dai *et al* demonstrated about 13 Å lattice polaron correlations at room temperature in $La_{1-x}Ca_xMnO_3$ [25]. Adams *et al* found $\sim$10 Å polaron correlations in $La_{0.7}Ca_{0.3}MnO_3$, which is weakly temperature dependent [26]. Such small clusters could act as nucleation sites for the larger-scale phase separation. The inhomogeneity that we proposed may be relevant to magnetoelectronic phase separation, and may be a universal phenomenon in these materials.

Our simulated atomic distribution and local structure could help some research workers further understand their experimental results and raise more theoretical research on the La-site doping effect. Recently, it was found that the charge ordering and phase separation seem to be general phenomena in some transition-metal oxides, for example, doped manganites or superconducting compounds [4]. Our results may be beneficial for the research of other transition-metal oxides.

4. Conclusion

Using the atomistic simulation technique, we studied the possible Sr cation distribution of $La_{1-x}Sr_xMnO_3$ at several different doping densities ($x = 1/18, 1/9, 1/6, 2/9$ and $1/4$). It is found that the Sr cluster of 5–15 Å in size is more structurally reasonable and energetically favourable than the random Sr distribution at low temperatures, and the Sr-rich domains may be a chemical representation of microscopic phase separation. The local structural disorders in the vicinity of clustered Sr and La ions are quite different and will be reduced by increasing doping densities. This nano-scale inhomogeneity may be a universal phenomenon existing in these materials. The impact of such nano-scale inhomogeneity should not be neglected for any

local theoretical treatment of these compounds, particularly in the context of magnetoelectronic phase separation.

Acknowledgments

The authors would like to thank the financial support of the Ministry of Science and Technology of China (TG2000067108 and 2002CB613500) and National Science Foundation of China (90401013).

References

[1] Dagotto E, Hotta T and Moreo A 2001 *Phys. Rep.* **344** 1
[2] Salamon M B and Jaime M 2001 *Rev. Mod. Phys.* **73** 583
[3] Ramirez A P 1997 *J. Phys.: Condens. Matter* **9** 8171
[4] Moreo A, Yunoki S and Dagotto E 1999 *Science* **283** 2034
[5] Shibata T, Bunker B, Mitchell J F and Schiffer P 2002 *Phys. Rev. Lett.* **88** 207205
[6] Louca D and Egami T 1999 *Phys. Rev.* B **59** 6193
[7] Perring T G, Aeppli G, Moritomo Y and Tokura Y 1997 *Phys. Rev. Lett.* **78** 3197
[8] Shen S-Q and Wang Z D 1998 *Phys. Rev.* B **58** R8877
[9] Hennion M, Moussa F, Biotteau G, Rodríguez-Carvajal J, Pinsard L and Revcolevschi A 1998 *Phys. Rev. Lett.* **81** 1957
[10] Arovas D P, Gómez-Santos G and Guinea F 1999 *Phys. Rev.* B **59** 13569
[11] Catlow C R A and Price G D 1990 *Nature* **347** 243
[12] Gale J and Rohl A L 2003 *Mol. Simul.* **29** 291
[13] Catlow C R A, Islam M S and Zhang X 1998 *J. Phys.: Condens. Matter* **10** L49
[14] Bourova E, Parker S C and Richet P 2000 *Phys. Rev.* B **62** 12052
[15] Tang F L and Zhang X 2006 *Phys. Rev.* B **73** 144401
[16] *Natl. Bur. St., 1972 [U.S.] Monogr. 25, 10, 58*
[17] Dabrowski B, Xiong X, Bukowski Z, Dybzinski R, Klamut P W, Siewenie J E, Chmaissem O, Shaffer J, Kimball C W, Jorgensen J D and Short S 1999 *Phys. Rev.* B **60** 7006
[18] Chmaissem O, Dabrowski B, Kolesnik S, Mais J, Jorgensen J D and Short S 2003 *Phys. Rev.* B **67** 094431
[19] Chatterji T, Ouladdiaf B, Mandal P, Bandyopadhyay B and Ghosh B 2002 *Phys. Rev.* B **66** 054403
[20] Guo Y, Zhang X and Wäppling R 2000 *J. Alloys Compounds* **306** 133
[21] Tang F L and Zhang X 2005 *J. Phys.: Condens. Matter* **17** 6507
[22] Zhao G M, Conder K, Keller H and Müller K A 1996 *Nature* **381** 676
[23] Heffner R H, Sonier J E, MacLaughlin D E, Nieuwenhuys G J, Ehlers G, Mezei F, Cheong S-W, Gardner J S and Röder H 2000 *Phys. Rev. Lett.* **85** 3285
[24] Teresa J M D, Ibarra M R, Algarabel P A, Ritter C, Marquina C, Blasco J, García J, Moral A D and Arnold Z 1997 *Nature* **386** 256
[25] Dai P, Fernandez-Baca J A, Wakabayashi N, Plummer E W, Tomioka Y and Tokura Y 2000 *Phys. Rev. Lett.* **85** 2553
[26] Adams C P, Lynn J W, Mukovskii Y M, Arsenov A A and Shulyatev D A 2000 *Phys. Rev. Lett.* **85** 3954